

## Forum C Rare Earth, Vanadium and Titanium Materials

### C01(Invited)

#### Progress of Multimetal Resources for Hydrometallurgical Cleaner Production Technology

Tao QI, Jingkui QU, Lina WANG

National Engineering Laboratory for Hydrometallurgical Cleaner Production Technology,  
Institute of Process Engineering (IPE), Chinese Academy of Sciences (CAS)

**Abstract:** Ti, V, Zr and Ni are important strategic metals which have wide applications in chemicals, electronics, steel, military, aeronautics and astronautics Fields. Several novel green manufacturing processes have been developed to utilize vanadium-bearing titanomagnetites, laterite ores and zircon sand efficiently. Titanium slag, rutile type of  $\text{TiO}_2$ , titanium suboxide, vanadyl sulfate solution, high purity  $\text{V}_2\text{O}_5$  were successfully prepared using selective reduction and hydrometallurgy methods. The method of “atmospheric pressure acid leaching- selective hydrolysis- green separation of Ni and Co from impurities” for processing laterite ores was developed. A new technology of cleaner production of zirconium oxychloride was developed, including continuous and efficient decomposition of zircon sand by alkaline molten salt, clean separation technology of impurities and comprehensive utilization of waste alkali liquid and silicon sol. The resource utilization efficiency was greatly improved, while the energy consumption and the waste emission were decreased.

### C02(Invited)

#### Research Developments of Rare Earth Magnetic Materials Based on Rare Earth Resources of PanXi Area

Ying Liu

Materials Science and Engineering College, Sichuan University

Based on the Rare Earth resources of Panxi area, high-performance rare earth permanent magnetic materials were obtained by the rapid quenching-heat treatment, hot press-hot deformation and powders metallurgy sintering, respectively. The phase composition, phase content, grain morphology and grain size were investigated by means of XRD, SEM, TEM and Mossbauer, etc. The correlation between microstructure and magnetic properties of the materials were established. Progress were drawn as follows:

A complete set of key equipment of continuous rapid quenching for amorphous NdFeB and

rapid crystallization at high temperature were developed. Nano-crystallized NdFeB magnetic powders with high performance can be produced at a large scale continuously. The maximum magnetic energy product was 129kJ/m<sup>3</sup>. The partial replacement of NdPr alloy by Ce could lead to the reduction of grain size and more regular grain morphology of the quenched powders. Thus the dilutive effect to magnetic properties caused by Ce was weakened.

A new technology for obtaining highly-density composite permanent magnetic devices was developed. After compression molding, the density of the samples was 6.5g/cm<sup>3</sup> and the maximum magnetic energy product was 105kJ/m<sup>3</sup>. By adjusting the volume percent of the quenched NdFeB powders, multiple-poles PPS/NdFeB composite permanent devices were obtained by injection molding. The magnetic field strength on the surface was 161.1 mT. With Ce-riched quenched powders, low-cast composite permanent magnetic devices were prepared. When the substituted amount of PrNd alloys by the Ce was varied from 20wt% to 70wt%, the maximum magnetic energy product of molded components and injection molding components were 5.0-8.5MGOe and 3.0-5.0MGOe, respectively.

We have clarified the microstructure evolution of anisotropic hot deformed NdFeB magnets, mastered the method of microstructure control, designed and manufactured the key equipment of induction hot pressing, batch produced the anisotropic magnets with the maximum energy product of 45.0-51.0MGOe. A new hot deformed magnets crushing method combined axially oriented coarse crushing and fine milling was developed on the crush of the deformed magnets. The performances of crushed anisotropic powders were better than MQA-38-14 powders produced by the Magquench Corp. Meanwhile, a new idea of applying hot deformation in the process of desorption and recombination of the disproportionated nano-crystalline Nd-Fe-B powders was suggested, The nano-scaled Nd<sub>2</sub>Fe<sub>14</sub>B grains could nucleate and orientated grow in the desorption and recombination reaction under the pressure. It obtained nanocrystalline Nd-Fe-B magnets with uniform grain size and good degree of texture. Based on the low melting point of Ce, hot densification temperature reduced significantly and good orientation of the microstructure could obtain after hot deformation. When the proportion of Ce instead of the (Pr,Nd) above 20wt%, the maximum energy of anisotropic Ce-rich magnets can achieve 32.3MGOe.

A new kind of Ce-rich inter-granular phase was designed and Ce-rich sintered magnets with multi main-phases coupled were constructed. Strips casting technology, ultrafine grinding technology, magnetic field molding and sintering techniques of the Ce-rich alloy with low oxygen content were researched. We have prepared cost-effective Ce-rich rare earth permanent magnets, which the proportion of Ce instead of the (Pr,Nd) is 20wt%-30wt%, the coercivity could

achieve 7.0-9.0kOe, the maximum energy could surpass 35MGOe.

### C03

#### Effects of Charge Compensators on Structure and Luminescent Properties of Microwave Synthesized $\text{CaMoO}_4:\text{Eu}^{3+}$ Red Phosphors

Ying Han, Zhi-lin Li, Wan Zhang, Yan-jie Yin, Yan-mei Li, Li-li Wang, Yong-qing Zhai\*

College of Chemistry and Environmental Science, Hebei University, Baoding 071002, China

\*Corresponding author: e-mail: zhaiyongqinghbu@163.com

**Abstract.** Red phosphors  $\text{CaMoO}_4:\text{Eu}^{3+}$  were synthesized by microwave method with  $\text{MnO}_2$  as microwave absorbent. The phase structure and luminescent properties of the as-synthesized phosphors were investigated by X-ray powder diffraction and Fluorescence spectrophotometer. The results show that when the reaction time was 40 min, microwave power was medium-high fire (~560 W), we got the tetragonal  $\text{CaMoO}_4:\text{Eu}^{3+}$  pure phase. The excitation spectrum of  $\text{CaMoO}_4:\text{Eu}^{3+}$  was composed by a broad band between 200 nm and 350 nm and a series of peaks from 350 nm to 500 nm. The main peak was at 305 nm. The emission spectrum was composed of a series of peaks in the range of 550~750 nm and the main peak was at 617 nm due to the  $^5\text{D}_0 \rightarrow ^7\text{F}_2$  transition of  $\text{Eu}^{3+}$ . Doping charge compensator  $\text{Li}^+$ ,  $\text{Na}^+$  or  $\text{K}^+$  could improve the luminous intensity of the sample. When the doping amount of  $\text{Li}^+$ ,  $\text{Na}^+$  or  $\text{K}^+$  were 8 mol%, the luminous intensity of the sample reached the maximum. The intensity of the emission peak at 617 nm was 4.04, 3.42, 3.48 times of sample without doping charge compensator.

**Key words:** Microwave method,  $\text{CaMoO}_4:\text{Eu}^{3+}$ , Red phosphors, Charge compensator.

### C04

#### Microstructural Modification of Ti-29Nb-13Ta-4.6Zr for Implant Applications

Q. Zhou<sup>1</sup>, G. Itoh<sup>2</sup>, M. Niinomi<sup>3</sup>

1 College of Mechanical and Electrical Engineering, Nanjing University of Aeronautics and Astronautics, Nanjing, China, 210016

2 Department of Mechanical Engineering, Ibaraki University, Ibaraki, Japan, 316-8511

3 Department of Biomaterials Science, Institute for Materials Research, Tohoku University, Sendai, Japan, 980-8579

A new near-beta titanium alloy was developed for biomaterial applications by a research group from Japan, which composition is approximately 29 Nb, 13 Ta and 4.6 (wt %) Zr. This alloy

has higher biocompatibility with lower elastic modulus compared to that of Ti-6Al-4V. The design of the alloying was based on the values of the bond order  $\bar{B}_o$  which is the measurement of the covalent bond strength between titanium and an element and the d-orbital energy level  $\bar{M}_d$  which is correlated to the electronegativity and the metallic radius of elements. For lowering elastic modulus, higher values of  $\bar{B}_o$  and  $\bar{M}_d$  are needed. However, for the stability of beta alloy, a higher  $\bar{B}_o$  and a lower  $\bar{M}_d$  are necessary. Finally, such elements and compositions were determined by the requirement for inducing integrated performance of high mechanical properties, nontoxicity and lower elastic modulus to the alloy.

The microstructure of solution-treated Ti-29-13 (Ti-29-13 is referred as the alloy of Ti-29%Nb-13%Ta -4.6%Zr) is equiaxial grain. However a hot-forged Ti-29-13 showed severe band-like transgranular structure, which weakens the mechanical properties of the alloy. By using backscattered electron images in the SEM and energy dispersive X-ray spectroscopic in SEM, it is found that the light part of the band structure is composed mainly of relatively light atom such as Ti, while the dark part of the band structure is composed mainly of relatively heavy Nb and Ta atoms. Segregation of beta stabilizer takes place in the as-received state (hot-forged). The beta stabilizer segregation remains after a cold-rolling or a solution treatment at 750°C for 4 hour. Thermomechanical processing was carried out to attempt to diminish the band structure. After repeated solution treatment and cold-rolling three times, dramatic reduction of the segregation band was found when comparing to that of the single annealing at 750°C for 4 h. Constant strain rate tensile tests at high temperatures were performed for the Ti-29-13 with modified microstructure. The improvement of the strain to failure of the Ti-29-13 has been confirmed with STCR3 treatment. However, band structure appeared again after high temperature deformation, the appearance of cavities concentrated on the dark band indicates more deformation takes place in this area. Different flow stresses between the light and the dark bands are accounted to this phenomenon.

## C05

### **Synthesis and Photoluminescence Properties of $\text{Sc}_{0.88-x}\text{Lu}_{0.05}\text{VO}_4:\text{Eu}^{3+}_{0.07},\text{Bi}^{3+}_x$ Red Phosphor**

**WU Di<sup>1,2</sup>, YE Xinyu<sup>1,3</sup>, ZHOU Jian<sup>1,2</sup>, WEN Xiaoqiang<sup>1,2</sup>, YANG Xinhua<sup>1,2</sup>, XIE Shiyong<sup>1,2</sup>**

(1. National Engineering Research Center for Ionic Rare Earth, Ganzhou 341000, Jiangxi, China ;  
2. Ganzhou Nonferrous Metallurgy Research Institute, Ganzhou 341000, Jiangxi, China; 3. School of Metallurgy and Chemistry Engineering, Jiangxi University of Science and Technology, Ganzhou 341000, Jiangxi, China; )

$\text{Sc}_{0.88-x}\text{Lu}_{0.05}\text{VO}_4:\text{Eu}^{3+}_{0.07},\text{Bi}^{3+}_x$  ( $0 \leq x \leq 0.05$ ) red phosphors were synthesized by solid state reaction at  $1200^\circ\text{C}$  for 3h. The structure, morphology and luminescence spectra of samples are investigated by X-ray diffraction (XRD), Scanning electron microscope (SEM) and fluorescence spectrophotometer, respectively. The samples doped with  $\text{Eu}^{3+}$ ,  $\text{Lu}^{3+}$  and  $\text{Bi}^{3+}$  maintain the body-centered tetragonal structure of  $\text{ScVO}_4$  and the morphology remains essentially unchanged with slight agglomeration. The excitation spectrum of  $\text{Sc}_{0.88-x}\text{Lu}_{0.05}\text{VO}_4:\text{Eu}^{3+}_{0.07},\text{Bi}^{3+}_x$  emerged redshift and the excitation intensity increase within the near UV excitation (360-400nm). The optimum doping concentration of  $\text{Bi}^{3+}$  is 0.02(x value), and the maximum emission intensity of  $\text{Sc}_{0.86}\text{Lu}_{0.05}\text{VO}_4:\text{Eu}^{3+}_{0.07},\text{Bi}^{3+}_{0.02}$  is higher than 88 % in comparison with  $\text{Sc}_{0.88}\text{Lu}_{0.05}\text{VO}_4:\text{Eu}^{3+}_{0.07}$  under 365 nm excitation. Decay curve of  $^5\text{D}_0$  state for as-prepared samples fits the single order exponential behavior, the lifetime of  $^5\text{D}_0$  increase first and then decrease with the increase of  $\text{Bi}^{3+}$  doping concentration. The internal quantum efficiency is up to 74% under 365nm excitation; When the temperature raises to  $200^\circ\text{C}$ , the emission intensity maintains 79% of that in the room temperature.  $\text{Sc}_{0.86}\text{Lu}_{0.05}\text{VO}_4:\text{Eu}^{3+}_{0.07},\text{Bi}^{3+}_{0.02}$  phosphor show high internal quantum efficiency and thermal stability, which is suitable for the UV-pumped white LED as red phosphor.

**Key words:** White LED, Red phosphor, Solid state reaction, Luminescence

## C06(Invited)

### A Review - The Properties and Applications of Nano-structured Titanium Oxide Materials

**Xiaoping Wu**

Pangang Group Research Institute Co., Ltd

With the unique optical properties, titanium dioxide ( $\text{TiO}_2$ ) has been widely used as a white pigment since early twentieth century. The numerous and diverse applications of  $\text{TiO}_2$  can be found in many common products such as paints, plastics, paper, sunscreens, ointments, etc. In the past decades, the emergence of nanotechnology and the discovery of some of the important application potentials of  $\text{TiO}_2$  have spurred the enormous interests to study  $\text{TiO}_2$ , particularly, nano-structured  $\text{TiO}_2$ , as functional materials. Since then, substantial advances have been made in the fabrication, characterization, fundamental understanding of  $\text{TiO}_2$  nano-materials, and their promising applications in a number of areas such as energy and environment. This review will discuss the properties of nano-structured  $\text{TiO}_2$  and highlight the recent development of their applications.

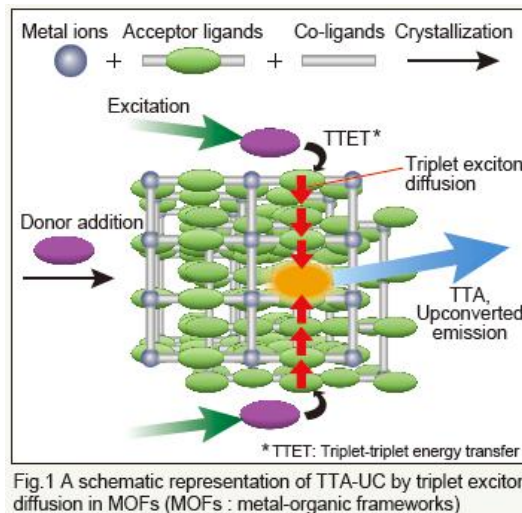
## C07

# High sensitivemethod for measuring Up conversion material

Jize Zhang

Hamamatsu Photonics (China) Co.,Ltd.

Photon up conversion is a technique for converting lower energy light into higher energy light. Triplet-triplet annihilation up conversion (TTA-UC) has a great amount of attention as one of those techniques which efficiently utilize light as weak as sunlight.



We will introduce a new method and device to measure up conversion material. That's will be very useful for functional material researching.

## C08

### New Preparation Technology of TiAl-based Multicomponent Alloys Using Aluminothermic Reduction with Compact Process by Titanium Sources in PanZHiHua

Shaoli YANG

School of resources and environmental engineering ,Panzhuhua University

There are rich resources of Titanium in the area of Panzhuhua and Xichang, but most of them do not get efficiently utilized. Because the sulphate titanium slag produced by the factories in Panzhuhua has a higher amount of calcium and magnesium compared with the high-titanium slag, it is not directly used to produce titanium sponge and titanium dioxide which is produced by chlorination process but used as raw material to prepare titanium dioxide produced by sulfuric process, such a process results to serious environmental pollution. Ti-Al master alloys have lots of excellent performances, which can be described as low density, high specific strength and thermostability etc., thus it received considerable attention as high temperature structural materials, so how to achieve better comprehensive utilization of titanium resources in Panzhuhua and Xichang and develop a environmentally friendly, efficient, energy saving and simple method to prepare Ti-Al based alloys has attracted much attention from the scientists. In this report, the

sulphate titanium slag was used as raw material to prepare Ti-Al based alloys by aluminothermic reduction, and the focus was mainly on the problem that the slag could not be separated easily and conveniently, which was studied and explored seriously.

Experiments about the separation of slag and alloy showed that the degree of separation could reach 92.66% by adjusting the ratios of the reactants, controlling the temperature, and changing heat preservation time. We also got that the degree of separation and alloy aggregation were better when the compositions of the slag were close to C-type slag (the slag system that  $\text{CaO}/\text{Al}_2\text{O}_3$  equals 0.8). And the phases composition of the Ti-Al based alloys were Ti-Si, Ti-Al-Fe and Ti-Al, in addition, the oxygen in the alloy was mainly from  $\text{SiO}_2$ , titanium oxide and some inclusion of  $\text{Al}_2\text{O}_3$ . The oxygen in the alloy could reduce to less than 2% by controlling the parameters, and refinement needed to be done to reduce the oxygen content in the alloy.

Our team refines coarse TiAl alloy by vacuum magnetic levitation melting furnace, the purpose is that we can remove the inclusion and gas in the alloy, reduce the impurity content and improve performance of the alloy.

The results for refining were as follows: when the melting current is 60A and holding time is 5 minutes, the content of inclusions in the alloy declined by 45%. The large inclusion particles in the alloy is removed (particle size  $>5\mu\text{m}$ ), but there are small particles inclusion (particle size  $<5\mu\text{m}$ ). Before and after refining the alloy mainly have  $\text{TiAl}_2$  or  $(\text{TiAl}/\text{TiAl}_3)$ ,  $\text{Ti}_5\text{Si}_3$ ,  $\text{Ti}_2\text{Al}$ , TiAl and other solid solution of Si, Mn, and Fe. The cooling rate has little influence on the removal efficiency, but it has great influence on the organization. When the cooling speed is 10A/5min, alloy is mainly  $\gamma$  and  $(\gamma/\alpha_2)$  phase and it has a high plasticity and strength. After refining alloy density decreased, and decreases with the decrease of the cooling rate of alloy density. The hardness of alloy increases after refining, with the decrease of the cooling rate of alloy hardness decreases as a whole.

## C09

### **Preparation of Synthetic Rutile from Titania Slag during Microwave Roasting and Industry Application**

**Guo Chen, Professor**

Yunnan Minzu University

Because of the shortage of natural rutile, synthetic rutile is widely used as substitute raw materials for natural rutile owing to its excellent mechanical and thermal properties. In the present study, sulphate titanium slags were prepared from ilmenite ore by carbon thermal reduction, and were chosen as the research objects. Study on the characteristics and structure of

sulphate titanium slag, and combine with the traditional features of microwave energy transmission and selective microwave heating, and mechanism research and regulatory mechanism of preparing synthetic rutile under microwave heating were investigated. The effects of the physicochemical properties of sulphate titanium slags on the complex dielectric constant of raw materials, and microwave selective heating on the interaction mechanism of selectivity enrichment and reaction kinetic parameters of microwave roasting sulphate titanium slags were characterized using theory analysis, experimental research and characterization. The mechanism of heat and mass transfer on reaction during microwave heating was analyzed, and the crystal structures, microstructure and particle size distributions of microwave treated synthetic rutile were systematically investigated. The demonstration of microwave heating techniques can be applied effectively and efficiently to the treatment processing of synthetic rutile with theoretical basis.

## **C10(Invited)**

### **Application of Rare Earths in Chemical Process Intensification**

**Zuohua Liu, Professor**

Chongqing University

The chloroprene manufactured by acetylene method including monomer chloroprene generation and chloroprene polymerization, and dimerization of acetylene in Nieuwland catalyst to produce monovinylacetylene (MVA) is a key operation unit for neoprene rubber manufacture in acetylene route. But acetylene has low solubility in traditional catalyst, and is prone to react with MVA to form divinylacetylene (DVA) and other byproducts, which harms to economic cost. In order to solve these problems, the modified Nieuwland catalyst obtained by adding graphene, graphene oxide and ionic liquid would improve the catalyst activity and regulate the acetylene dimerization process route. In addition, this work also introduced ultrasonic in the catalytic system to intensify the catalyst performance.

In the industrial electrolytic manganese processes, the energy consumption is closely related with electrolytic manganese oxide on the anode. The main development direction of electrolytic manganese technology is to reduce energy consumption and make a reality of energy saving and emission reduction. In this study, we import a little chloride ion or rare earth ion to the traditional system of manganese sulfate, investigating the influence of chloride ion or rare earth ion about electrochemical oscillations on the anode.

**Key words:** acetylene dimerization; graphene; graphene oxide; ionic liquid; ultrasonic;



electrolytic manganese processes; chloride ion; rare earth ion

## C09(Invited)

### C11

#### Study on Photocatalytic Reduction of Cr(VI) by Fluorine-Doped TiO<sub>2</sub>

Shu-qin WANG<sup>1,a</sup>, Bo BI<sup>1</sup> and Xue-juan ZHAO<sup>1</sup>

<sup>1</sup>School of Environmental Science and Engineering,  
North China Electric Power University, Baoding 071003, China.

<sup>a</sup>E-mail: wsqhg@163.com

To enhance the photocatalytic performance of nano TiO<sub>2</sub> on Cr(VI) reduction, we have prepared fluorine-doped TiO<sub>2</sub> photocatalyst (named as F-TiO<sub>2</sub> hereinafter) via sol-gel method. N-doped TiO<sub>2</sub> (N-TiO<sub>2</sub>) was also prepared for comparison. XRD, BET and UV-vis DRS were used to characterize and analyze these samples. The photocatalytic activity of different photocatalysts was evaluated by Cr(VI) reduction experiments. Effects of preparation conditions, reaction kinetics and catalyst lifetime were discussed in this paper. The experimental results showed that the best preparation conditions were as follows: ammonium fluoride used as F source, F/Ti=0.1, calcination temperature=500°C and calcination time=3h. The photocatalytic reduction process conformed the first-order kinetics, and the reaction rate constant of F-TiO<sub>2</sub> was 4 times as large as that of virgin TiO<sub>2</sub>. Characterizations also proved that F doping improved the photocatalytic activity of TiO<sub>2</sub>.

**Keywords:** Sol-gel method, Fluorine-doped TiO<sub>2</sub>, Photocatalytic reduction, Cr(VI)

### C12

#### New Thorium-Free Long-Wave Infrared Low-Index Evaporation

##### Materials: BaF<sub>2</sub>-ReF<sub>3</sub> (Re=La, Pr, Er, Sm)

Bin Li

Shanghai Institute of Technical Physics, Chinese Academy of Sciences

Thorium fluoride (ThF<sub>4</sub>) is an infrared coating material with excellent optical and mechanical properties. However, the natural radioactivity of thorium leads to forbidding its usage. The continuing search for alternate non-radioactive substitutes is a main topic among the coating materials scientists worldwide. Investigation into the admixture of rare earth fluorides with other fluorides will be an important solution.

It was disclosed that the admixture of four rare earth fluorides, LaF<sub>3</sub>, PrF<sub>3</sub>, ErF<sub>3</sub> and SmF<sub>3</sub> with BaF<sub>2</sub>, has the optimal optical and mechanical properties. Moreover, it was also observed

that the intrinsic stress in the mixed fluoride films is not reduced with the increasing ionic radius of the admixed fluorides, as proposed by S. F. Pellicori. An explanation for the stress behavior was suggested that alkaline earth fluorides on the grain boundaries of rare earth fluorides have a lower surface energy than rare earth fluorides, hence, the inter-grain forces of rare earth fluorides are reduced, according to the grain boundaries model.

Consequently, four environment-harmonious, smoothly evaporated, mixed infrared low-index evaporation materials with reduced stress, Thfree1, Thfree2, Thfree3 and Thfree4, were developed. It can be found that the thin films evaporated from Thfree1 and Thfree2 have a superior spectral transmittance to that evaporated from IR-F625, a patented products owned by Umicore Thin Film Products, and, that evaporated from evaporation materials of  $\text{YbF}_3$ , which was manufactured by Umicore Thin Film Products and is currently used in the infrared broadband antireflection coatings on the windows in satellite-borne remote-sensing instrument. In addition, they were also testified to be robust enough to withstand the rigors of use in spaceflight. Furthermore, the performance of infrared broadband antireflection coatings fabricated using Thfree1 and Thfree2 approached that using  $\text{ThF}_4$ . Therefore, an infrared coating materials with independent intellectual property rights was developed in order to replace the expensive imported goods, and provided a solution to the critical technical problem in satellite-borne remote-sensing: shortage of environment friendly, robust, long-wave infrared low-index evaporation materials.

## **C13**

### **Low cost preparation of $\text{TiO}_2$ nanoparticles via thermal decomposition and their photoelectrochemical properties**

**Jie Zhang, and Siyu Tang, and Qinghong Zhang**

State Key Laboratory for Modification of Chemical Fibers and Polymer Materials, College of Materials Science and Engineering, Donghua University, Shanghai 201620, P. R. China

Corresponding author. Tel: +86-21-67792943; fax: +86-21-67792855. E-mail address:

[zhangqh@dhu.edu.cn](mailto:zhangqh@dhu.edu.cn) (Q. H. Zhang)

One-step route based on the thermal decomposition of the double salt  $(\text{NH}_4)_2\text{TiO}(\text{SO}_4)_2$  (ammonium titanyl sulfate, ATS) is presented to prepare size-defined aggregates of Ti-based nanoparticles with structural hierarchy. The phase composition of  $\text{TiO}_2$  nanoparticles was depended on the atmospheres and reaction temperatures. In air and temperatures ranged from 600 to 900 °C, the samples were in anatase phase, but a longer duration was needed to complete

ATS decomposition. However, in flowing Ar gas, the samples were in predominant rutile phase at the temperature as low as 700 °C. The as-prepared TiO<sub>2</sub> powders were characterized by X-ray diffraction analysis (XRD), transmission electron microscopy (TEM), UV-vis diffuse reflectance spectra (DRS), and BET surface area techniques. The network of anatase TiO<sub>2</sub> with a specific surface area up to 64 m<sup>2</sup>/g contains large mesopores with a mean diameter of ca. 15 nm, and the large pore size allows more accessible surface and interface available for the photocatalytic degradation of large-molecule dyes. The photocatalytic activity of the prepared TiO<sub>2</sub> under UV light irradiation is compared to Degussa P-25 using the photocatalytic degradation of methylene blue (MB), and some larger molecular azo dyes as the model reactions. The anatase TiO<sub>2</sub> nanoparticles derived from one-step route show the highly efficient photocatalytic activity for the degradation of dyes in comparison with Degussa P-25.

Also, TiO<sub>2</sub> nanocrystals derived from hydrothermal method were widely used as the photoanodes of dye-sensitized solar cells (DSSCs). Moreover, TiO<sub>2</sub> nanoparticles from ATS calcined at 700 °C with a faster heating rate (5 °C/min) had a wider pore size distribution and exhibited a higher light scattering abilities, while the ones from those calcined at a slower heating rate (3 °C/min) had a narrow pore size distribution but possessed a higher specific surface area (72.8 m<sup>2</sup> g<sup>-1</sup>) for adsorbing more dye. The DSSC based on two kind of TiO<sub>2</sub> nanoparticles as the photoelectrode all exhibited an excellent short-circuit current density (15.21 mA cm<sup>-2</sup> and 15.94 mA cm<sup>-2</sup>) and a highly efficient power conversion efficiency (7.78% and 8.16%).

**Keywords:** Powders-chemical preparation; TiO<sub>2</sub> nanoparticles; Dye-sensitized solar cells; Photocatalytic

## C14

### **Study on the Hydrolysis Process of Low Concentration Titanyl Sulfate Solution**

**Dongmei Luo, Fanbo Zeng, Li Fu, Zhao Zhang, Bin Liang, Dan Li**

College of Chemical Engineering, Sichuan University, China

Waste Acid solution is the by-product came from hydrolysis process of titanyl sulfate solution. In order to decrease the pollution of acid waste water and production costs the waste acid solution should be recycled utilized. Then low concentration titanyl sulfate solution is obtained in the recycling process. The hydrolysis process of low concentration titanyl sulfate solution without adding external seeds was studied in this paper by analyzed the behavior of sulfur in process. And also alternating-electric field was employed in the research. The analysis

and methods of thermogravimetric-differential scanning calorimetry (TG-DSC), energy dispersive spectrometer (EDS), Fourier transform infrared spectroscopy (FTIR), X-ray diffraction (XRD), UV-Vis diffuse reflectance spectra and Raman spectroscopy were employed to characterize. Based on the results of structure and morphology of the hydrolysis product and product of  $\text{TiO}_2$ , the hydrolysis process of low concentration titanium sulfate solution was illustrated.

**Keywords:** low concentration titanium sulfate; hydrolysis; sulfur; alternating electric field

## C15

### Structure and Catalytic Performance of Supported Perovskite Materials for Methane Catalytic Combustion

Hang-yu Du<sup>a</sup>, Xiang Gao<sup>b</sup>, Yun-fei Si<sup>c</sup>, Jun-ge Zhang, Zhong-ping Yang, Ruisheng Hu

School of Chemistry and Chemical Engineering, Key Laboratory of Rare Earth Materials, Inner Mongolia University, Hohhot 010021, Inner Mongolia, PR China

Email<sup>a</sup>: huruisheng@126.com, Email<sup>b</sup>: gaoxiang0213@sina.cn, Email<sup>c</sup>: 1002066352@qq.com

Corresponding author Ruisheng Hu. Email: cehrs@imu.edu.cn ; Tel: +86-138-4713-6021.

Methane catalytic combustion has been attracting extensive attention on for its energy conservation and emission reduction, instead of the conventional flame combustion, catalytic combustion could significantly lower the light-off and complete oxidation temperature, leading to efficiently decrease of  $\text{NO}_x$  emission. Although perovskite oxides catalysts have been frequently used for methane combustion, only a few works have been reported on the catalytic properties of supported double perovskites.

Biphasic intergrowth  $\text{La}_2\text{MnCuO}_6$  and  $\text{La}_2\text{MnCuO}_6\text{-Al}_x\text{Mg}_{1-x}\text{O}$  ( $x=0, 1/11, 2/12$  and  $3/13$ ) composite oxide (30 wt%  $\text{La}_2\text{MnCuO}_6$  loading) were successfully prepared by the sol-gel method using glucose as complexing agent. The obtained catalysts were evaluated for methane catalytic combustion after calcined at 1100 °C for 3 h. The characterization methods include XRD, BET, SEM, TEM, M-H, and XPS.

All diffraction peaks in XRD figure belong to  $\text{La}_2\text{MnCuO}_6$  without impurity peaks. Pure double perovskite structure has formed in  $\text{La}_2\text{MnCuO}_6\text{-Al}_x\text{Mg}_{1-x}\text{O}$  ( $x=2/12$ ) while  $\text{La}_2\text{MnCuO}_6\text{-MgO}$  supported composite oxide has formed in sample  $\text{La}_2\text{MnCuO}_6\text{-MgO}$  &  $\text{La}_2\text{MnCuO}_6\text{-Al}_x\text{Mg}_{1-x}\text{O}$  ( $x=1/11$ ). With molar content of Al increasing, samples  $\text{La}_2\text{MnCuO}_6\text{-MgO}$  &  $\text{La}_2\text{MnCuO}_6$  showed stronger signals of  $\text{MgAl}_2\text{O}_4$  spinel phase.

On the other hand,  $\text{La}_2\text{MnCuO}_6\text{-Al}_x\text{Mg}_{1-x}\text{O}$  ( $x=1/11$ ) exhibited significantly improved catalytic activity ( $T_{10}=418.7$  °C,  $T_{90}=624.7$  °C) compared with that of  $\text{La}_2\text{MnCuO}_6$ , whose  $T_{10}$  decreased by 66 °C and  $T_{90}$  decreased by 87.4 °C, respectively. The excellent catalytic activity of

$\text{La}_2\text{MnCuO}_6\text{-Al}_x\text{Mg}_{1-x}\text{O}$  ( $x=1/11$ ) caused by the optimum  $\text{Al}^{3+}$  substitution for  $\text{Mg}^{2+}$  in  $\text{La}_2\text{MnCuO}_6\text{-Al}_x\text{Mg}_{1-x}\text{O}$  can be ascribed to the remarkable decline of the activation energy during the reaction, the larger number of adsorption oxygen on the catalyst surface, the significant elevation of the amount of  $\text{Mn}^{3+}$  ions.

The project was supported by the National Natural Science Foundation of China (No.21263008).

**Key Words:** Biphasic intergrowth, Supported perovskite, Methane catalytic combustion

## C16

### Structures and Luminescent Properties of $\text{M}_x\text{Ca}_{2-x}\text{SiO}_4\text{:Ce}^{3+},\text{Al}^{3+}$ (M=Mg,Sr,Ba) Phosphors

JIANG Jian-qing<sup>1</sup>, ZHOU Ming<sup>1</sup>, YANG Feng-li<sup>1\*</sup>, HOU De-jian<sup>1</sup>, YE Xin-yu<sup>1,2\*</sup>

(1. School of Metallurgy and Chemistry Engineering, Jiangxi University of Science and Technology, Ganzhou 341000, Jiangxi, China; 2. National Engineering Research Center for Ionic Rare Earth, Ganzhou 341000, Jiangxi, China)

A series of  $\text{M}_x\text{Ca}_{2-x}\text{SiO}_4\text{:0.5mol\%Ce}^{3+},4\text{ mol\%Al}^{3+}$  (M=Mg, Sr, Ba;  $x=0.05, 0.1, 0.15, 0.2$ ) phosphors was prepared by high temperature solid-state reaction. The structure, morphology and luminescent properties of the phosphors were studied by X-ray diffractometer, scanning electron microscope and fluorescence spectrometer. The results show that the structure of  $\gamma\text{-Ca}_2\text{SiO}_4$  phase maintains when  $x=0.05$  for  $\text{Mg}_x\text{Ca}_{2-x}\text{SiO}_4\text{:Ce}^{3+},\text{Al}^{3+}$  phosphor. Under the excitation of 450nm light, a broad band emission centered at 565nm is observed, which mainly corresponds to the  $5d\rightarrow^2\text{F}_{7/2}$  and  $5d\rightarrow^2\text{F}_{5/2}$  transitions of  $\text{Ce}^{3+}$ . When  $x$  grows up to 0.1-0.2, the phase is changed to  $\beta\text{-Ca}_2\text{SiO}_4$  with impurity phase. With the increase of the doping concentration, the emission peak of  $\text{Mg}_x\text{Ca}_{2-x}\text{SiO}_4\text{:Ce}^{3+},\text{Al}^{3+}$  shifts from 503nm to 423nm under the excitation of 365 nm. When  $x=0.05-0.15$  for  $\text{Sr}_x\text{Ca}_{2-x}\text{SiO}_4\text{:Ce}^{3+},\text{Al}^{3+}$  phosphor, the structure and luminescent properties are almost same as those of the Sr-free phosphor. When  $x=0.2$ , the phase is changed to  $\alpha'_H$ . Under the excitation of 365 nm, the emission peak locates at 465nm. When  $x=0.05-0.1$  for  $\text{Ba}_x\text{Ca}_{2-x}\text{SiO}_4\text{:Ce}^{3+},\text{Al}^{3+}$  phosphor, the structure and optical properties are almost unchanged, however, the phase transforms to  $\alpha\text{-Ca}_2\text{SiO}_4$  when  $x=0.15-0.2$ . The emission peak locates at 460nm under the excitation of 365nm. The reason for phase transformation and the change of luminescence properties of these phosphors are owing to the difference of melting points of alkali-earth metal oxides. The trend of phase transformation from  $\gamma\text{-Ca}_2\text{SiO}_4$  to other phases is enhanced with the doping from  $\text{Mg}^{2+}$  to  $\text{Sr}^{2+}$  and  $\text{Ba}^{2+}$ .

**Key words:**  $\text{Ca}_2\text{SiO}_4$ , alkaline-earth metal, phosphor, luminescence property

**C17**

## **Preparation and Magnetic Performance of Nanocrystalline SmCo<sub>12</sub>Si Alloy**

**Dong Liu, Dongxin Wang, Gang Hua, Xiaoyan Song\*, Haibin Wang and Xuemei Liu**

College of Materials Science and Engineering, Key Laboratory of Advanced Functional Materials, Education Ministry of China, Beijing University of Technology, Beijing 100124, China

\*e-mail: xysong@bjut.edu.cn

SmCo<sub>13-x</sub>Si<sub>x</sub> alloys with different silicon additions have been prepared. Nanocrystalline SmCo<sub>12</sub>Si alloy with single phase has been prepared for the first time based on a study of nanocrystalline SmCo<sub>13-x</sub>Si<sub>x</sub> alloys preparation. The structure refinement results show that the crystal structure of this alloy is TbCu<sub>7</sub>-type, which is the single phase after the sintering process below 600°C. With increasing of the sintering temperature of SPS, the density of the alloy increases, the grain size grows slightly, and the magnetic properties improve gradually. A small amount of FCC Co phase appeared in the sample after sintering process of 650°C.

**Keywords:** Nanocrystalline alloy; Sm-Co alloy; SPS; Metastable phase